Ain Shams Engineering Journal 13 (2022) 101748

Contents lists available at ScienceDirect

Ain Shams Engineering Journal

journal homepage: www.sciencedirect.com

Observer based rotor failure compensation for biplane quadrotor with slung load☆

Nihal Dalwadi [a], Dipankar Deb [a], S.M. Muyeen [b,*]

[a] Department of Electrical Engineering, Institute of Infrastructure Technology, Research and Management, Ahmedabad 380026, India
[b] Department of Electrical Engineering, Qatar University, Doha 2713, Qatar

ARTICLE INFO

Article history:
Received 24 December 2021
Revised 25 January 2022
Accepted 22 February 2022
Available online 14 March 2022

Keywords:
Biplane quadrotor
Slung load
Nonlinear Observer design
Partial Rotor failure
Wind gust
Trajectory tracking

ABSTRACT

In this study, mathematical modeling of biplane quadrotor with slung load is proposed. Performance of the biplane quadrotor is degrade while swinging of the slung load so to compensate it nonlinear observer based backstepping controller is designed that can not only handle the disturbance generated by the slung load but can also capable to tackle partial rotor failure and wind gust. Simulation study carried out by considering slung load swinging (only for quadrotor mode), wind gust, and rotor failure (for all three modes) as the external disturbance and nonlinear observer is design to estimate it. Backstepping control technique is used to design controller for all three modes of biplane quadrotor. Simulation study shows that proposed control scheme is cable to handle the disturbance generated by the different sources in quadrotor biplane.

1. Introduction

Unmanned Ariel Vehicles (UAVs) meant for agriculture, defense, e-commerce, payload delivery, photography, surveillance and inspection, wildlife monitoring, etc., use fixed-wings or rotary wings. However, a hybrid vehicle like a biplane quadrotor can take off and land like conventional rotary-wing UAVs and fly like fixed-wing UAVs and is helpful for all such purposes. Many researchers have worked to develop mathematical models and controller designs of the biplane quadrotor. Hrishikeshavan et al. [1] discussed the development of the quadrotor biplane. Swarnkar et al. [2] presented a flight dynamics model containing a comprehensive explanation of wing aerodynamics, prop wash modeling, and nonlinear controller design for the biplane quadrotor. Chipade et al. [3] presented a theoretical design and proof-of-concept flight demonstration of an innovative variable-pitch quadrotor biplane UAV conception for payload delivery. An evaluation study between modeling methods of a quadrotor biplane utilizes blade element theory to validate a reduced-order model that includes a simple interference model for trajectory planning and tracking simulation in [4]. Finally, Ryseck et al. [5] describe a morphing winglet for Quadrotor Biplane Tail-sitter (QBiT) to improve the efficiency within a broad flight envelope. Subsequently, mission-planning strategies are described and evaluated for QBiT vehicle in [6] with a folding winglet system in which the winglets offer two configurations that increase aerodynamic efficiency for different airspeed at the cost of increased airframe mass. Optimization-based trajectory planner developed and simulated by McIntosh et al. [7] for the independent transition of biplane quadrotor between hovering and level flight and vise versa. (see Fig. 1).

Biplane quadrotor couples the advantage of rotary-wing and fixed-wing UAVs to fly wing slung load while being in the quadrotor mode. Several researchers have worked on deriving the mathematical model of a slung load by combining its dynamics with aircraft [8,9]. Some have implemented advanced control algo-

Abbreviations: CoG, Center Of Gravity; DOB, Disturbance observer; DOBC, Disturbance Observer-based Control; ESC, Electronics Speed Controller; FD, Fault Detection; FTC, Fault Tolerant Control; IMU, Inertial Measurement Unit; LQR, Linear Quadratic Regulator; MPC, Model predictive control; NDO, Nonlinear Disturbance Observer; PI, Proportional Integral controller; PID, Proportional Integral Derivative; QBiT, Quadrotor Biplane Tail-sitter; SMC, Sliding Mode Control; UAV, Unmanned Aerial Vehicle.

* Corresponding author.
E-mail addresses: nihal.dalwadi.20pe@iitram.ac.in (N. Dalwadi), dipankarde-b@iitram.ac.in (D. Deb), sm.muyeen@qu.edu.qa (S.M. Muyeen).

☆ Peer review under responsibility of Ain Shams University.

Production and hosting by Elsevier

https://doi.org/10.1016/j.asej.2022.101748
2090-4479/

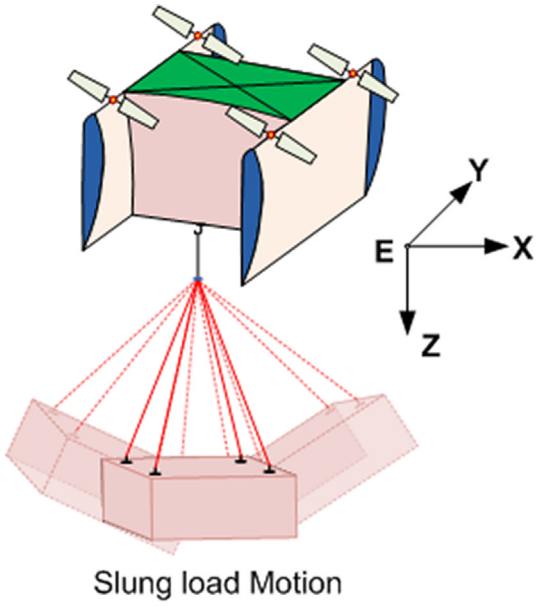

Fig. 1. Animated picture of biplane with slung load.

rithms for trajectory planning, tracking, optimization, and control of the slung load with quadrotor UAVs. Bisgaard et al. [10] presented the modeling and authentication of a generic slung load system using a small-scale helicopter for simulation, control, estimation, and pilot training. Notter et al. [11] derived a novel mathematical model for the multi-rotor with heavy slung load to implement a Model predictive control (MPC) scheme comparing the result with Linear Quadratic Regulator (LQR) control approach. The mathematical model of slung load integrates with the nonlinear model of helicopter. El.Ferik et al. present a backstepping controller with an anti-swing delayed feedback controller is designed for trajectory tracking through damping of the load oscillations [12].

Shirani et al. [13] presented a distributed controller for the supportive task consignment to multiple UAVs for load transportation with a marginal swing of slung load and the Udwadia-Kalaba method used for the mathematical model of the whole system. Yu et al. [14] presented a nonlinear backstepping controller for the quadrotor with slung load for trajectory tracking. de Angelis et al. [15] presented a filtering method established on a set of recursive equations which use available data from the onboard IMU without depending on an extra sensor and is applied to swing angle approximation for multicopter slung load application. Yihua et al. use Kane's method on an established mathematical model of a helicopter with an external load while considering the weight and flexibility of the cable in spring-mass-damper mode [16].

Disturbances and uncertainties widely exist in nonlinear underactuated systems like UAVs and adversely effect system performance, and stability [17]. A disturbance observer reconstructs the disturbance applied to the system (and can also estimate plant uncertainties) using measured output variables and known control input signals. Many researchers have studied and implemented a disturbance observer on a nonlinear system like a robotic arm, UAVs, etc. Disturbance observer adds robustness to the controller and is helpful with PID, Dynamic inversion control, backstepping control, sliding mode control, etc. Besnard et al. [18] developed a robust flight controller for a quadrotor by using the sliding mode control method with sliding mode disturbance observer to deal with external disturbance and model uncertainties. Chen et al. [19] proposed a novel nonlinear observer-based backstepping controller for a quadrotor to trajectory tracking. Chovancov et al. [20] implement different control methods like PD, LQR, and backstepping control design on quadrotor for improved performance despite external disturbances. Zhang et al. [21] propose an infinite-dimensional disturbance observer to approximation both the boundary disturbances and the distributed spatiotemporally varying disturbances in a flexible aircraft wing system. Disturbance observer-based tracking flight control scheme for unknown external disturbance estimation is developed [22].

Wind gusts, considered a strong disturbance for rotary-wing UAVs in hovering mode, are estimated using an observer that adds controller robustness. A high gain observer algorithm for online estimation and compensation of external disturbances like wind gusts is proposed [23]. Furthermore, Madani et al. [24] propose a novel approach of the backstepping control running parallel with a sliding mode observer for a quadrotor UAVs. Also, Zheng et al. [25] present a generalized disturbance observer (DOB) design framework motivated by iterative learning without requiring explicit plant inverse. Lyu et al. [26] present a disturbance observer (DOB) based method using H_∞ control technique to improve hovering accuracy in the presence of external disturbances such as crosswind. However, Li et al. [27] propose a robust nonlinear controller using H_∞ and nonlinear disturbance observer (NDO) to handle uncertainties in nonlinear terms, parametric uncertainties, and external disturbances in flight mode transition control of tail-sitter aircraft. Furthermore, Smith et al. [28] compare a baseline LQR controller to integral extension and Disturbance Observer-based Control (DOBC) with an anti-windup scheme to handle actuator saturation for external disturbances rejection. Finally, Castañed et al. [29] design attitude and airspeed controller for fixed-wing UAVs by using adaptive second-order sliding mode control that is robust despite external disturbances.

Shi et al. [30] design a high precision disturbance compensation scheme based on a harmonically extended state observer for attitude control of the quadrotor slung load system. Zheng et al. [31] present a nonlinear disturbance observer (DBO) based backstepping action and a dual power reaching law for a subsystem, and a multivariable sliding mode control structure for a second subsystem of quadrotor UAVs. The results are effective when compared with adaptive backstepping control. Recently, Dalwadi et al. [32] present a nonlinear disturbance observer-based backstepping control of tail-sitters to ensure trajectory tracking in the presence of wind gusts. Hou et al. [33] propose a terminal sliding mode fault-tolerant controller for a quadrotor with a total rotor failure considering model uncertainties along with the wind gusts. Li et al. [34] developed a disturbance observer and integral sliding mode technique-based fault-tolerant control subject to external disturbances and actuator failures. De.Crousaz et al. [35] present a generalized approach for (a) aggressive quadrotor maneuvering to pass through constrained regions with slung load, and (b) iterative optimal control with single and double rotor failure. Furthermore, a feedback linearization approach-based controller deals with a rotor failure condition in a quadrotor for trajectory tracking [36].

Lien et al. propose a flight control strategy using sliding mode control (SMC) of quadrotors under two-stage single rotor failure conditions: (a) fault detection (FD) and (b) fault-tolerant control (FTC), including a dual observer-based strategy [37]. Merheb et al. [38] developed an emergency PID-based fault-tolerant controller for quadrotor UAVs suffering total rotor losses with control reallocation among the healthy actuators. While Guzmán.Rabasa et al. [39] present a fault detection and diagnosis system under partial actuator faults in quadrotor UAVs with the rotation subsystem augmented by a robust linear parameter-varying observer for actuator fault detection. A model reference adaptive Control (MRAC) with PID helps develop a fault-tolerant controller [40], and elsewhere [41] three different MRAC methods: (a) Conven-

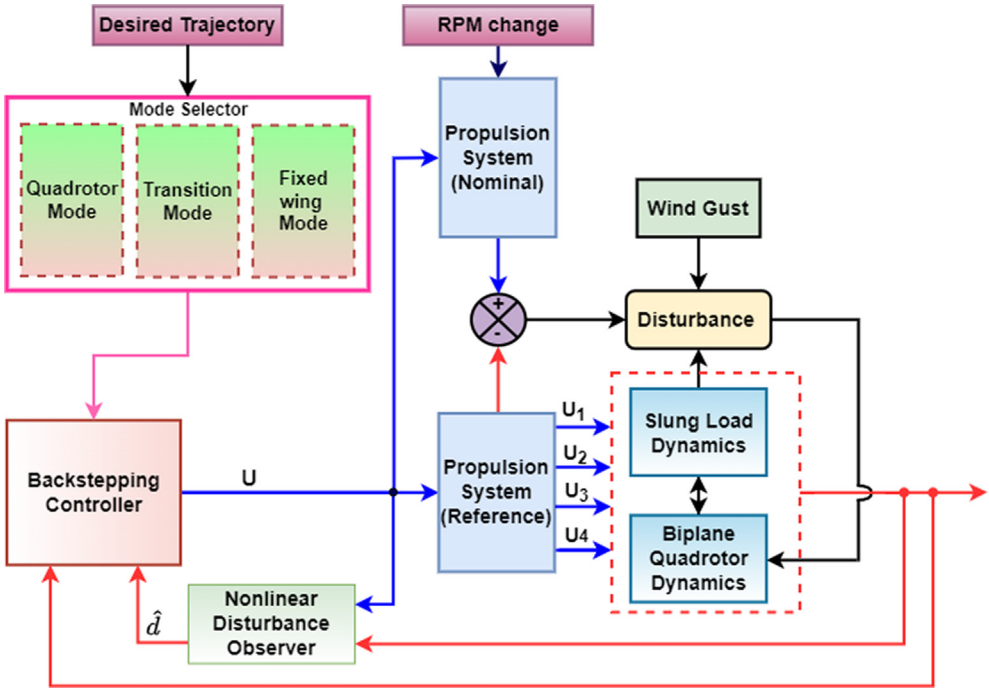

Fig. 2. Block Diagram of proposed Control Scheme.

tional MRAC, (b) MIT rule MRAC (c) Modified MRAC, handle a similar control problem. Lippiello et al. proposed a backstepping approach [42] and PID approach [43] to handle quadrotor propeller failures by turning off the motor opposite to the failed one, considering the quadrotor to be functioning in bi-rotor configuration for planned safe landing.

In this paper, we propose a biplane quadrotor model (quadrotor mode) with slung load and then design nonlinear observer to estimate the disturbances generated by the swinging of the slung load. We also design an observer-based backstepping controller for all three modes to remove the impact of wind gusts and disturbances due to partial rotor failure. Finally, we perform simulations using MATLAB Simulink with diverse possible scenarios for biplane quadrotor trajectory tracking with wind gusts and rotor failures. Biplane quadrotor has advantages of both rotary and fixed wing UAVs, and a better choice for payload delivery because while in the quadrotor mode, the payload is tied to biplane using cables. After payload drop, the biplane performs a transition maneuver to the level flight and flies to the original point while consuming less power than traditional quadrotors. The objectives of this work on quadrotor biplane are.

- Design an observer based backstepping controller for the biplane quadrotor with slung load for a desired trajectory tracking in presence of wind gusts and partial rotor failure (in quadrotor mode only).
- Observer design to estimate wind gust and rotor failure for all three modes.

In the next section, we derive a mathematical model of slung load, and then incorporate it with the dynamics of a biplane quadrotor.

2. Dynamical Model of a Biplane with Slung load

A biplane quadrotor augmented with slung dynamics is described in Fig. 2.

The desired trajectory is provided through a mode selector mechanism such that the backstepping controller is provided with an appropriate desired signal at the quadrotor, transition, or the fixed wing mode. Wind gusts are applied to the augmented biplane quadrotor. Nonlinear disturbance observer uses measured output state to find an estimated disturbance $\hat{d}$ provided to the controller. According to such estimated values, the measured output, and the input signal based on the modes, the backstepping controller generates the output U given to the propulsion system. The propulsion system consists of an Electronics Speed Controller (ESC) to provide the desired signals $[U_1U_2U_3U_4]$ to the respective motors for appropriate control of the biplane quadrotor. There is a change in the propeller's speed in partial rotor failure condition, calculated by the reference system and nominal system model. We consider wind gusts, partial rotor failure and the slung load swinging as the disturbances, and the nonlinear observer estimates it. For trajectory tracking study, we consider a spherical pendulum (slung) fixed at one point [44] with the origin of the slung load coordinates at the Biplane quadrotor's center of gravity (CoG).

2.1. Mathematical modeling of slung load

For a simplified and realistic dynamic model, we assume that.

- The Biplane quadrotor is a symmetrical and rigid body, and the CoG coinciding with the body fixed-frame origin is also the point of suspension.
- The cable is mass-less and the cable force is non-negative and non-negligible.

As shown in Fig. 3, the load does not swing above the lowest level of the biplane surface. For a cable of length L, by Pythagoras theorem, the slung load position about z-axis, $\zeta = \sqrt{L^2 - r^2 - s^2}$ is always non-negative for load positions s, r in y and x axes of inertial frame respectively. For the augmented system, Euler–Lagrange method helps compute the accelerations $\ddot{s}$ and $\ddot{r}$.

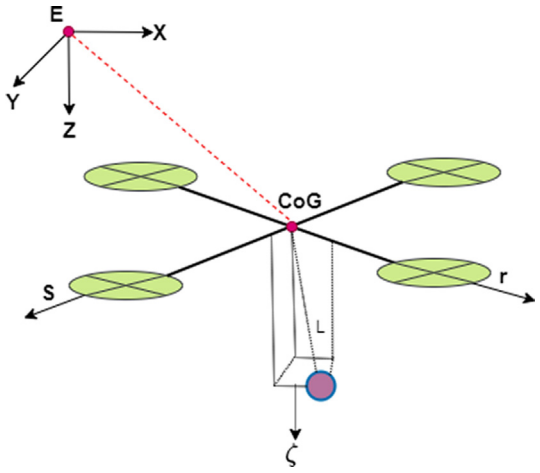

Fig. 3. Schematic of biplane quadrotor with slung load.

As per Newton's second law, the cable force between the Biplane and load equals the mass multiplying the absolute acceleration

$$d = \begin{pmatrix} d_x \\ d_y \\ d_z \end{pmatrix} = -m_l \begin{pmatrix} \ddot{x} + \ddot{r} \\ \ddot{y} + \ddot{s} \\ \ddot{z} + \ddot{\zeta} - g(\zeta/L) \end{pmatrix}, \tag{1}$$

where m_l is slung load mass, $\ddot{x}, \ddot{y}$ and $\ddot{z}$ are the acceleration components of biplane, and d_x, d_y, and d_z are the cable force components in x, y and z axis respectively, g is the gravitational constant, $\zeta, \ddot{\zeta}$ are the position and acceleration of slung load about z axis.

The suspended load at the CoG, affects only the translational, while the rotational motion remains the same. The cable force results in acceleration in the x, y and z directions. Typically, the payload and weight of the biplane quadrotor ratio is around $10-15\%$, and so if the biplane quadrotor weight is 18 kg then it can lift around 2 to 2.5 kg slung load in total.

2.2. Mathematical model of Quadrotor Biplane

Biplane dynamics [2], [46] are

$$\begin{bmatrix} \ddot{x} \\ \ddot{y} \\ \ddot{z} \end{bmatrix} = \frac{1}{m} \begin{bmatrix} F_{ax} \\ F_{ay} \\ -T + F_{az} \end{bmatrix} + g \begin{bmatrix} -s\theta \\ c\theta s\phi \\ c\theta c\phi \end{bmatrix} + \begin{bmatrix} rv - qw \\ pw - ru \\ qu - pv \end{bmatrix}, \tag{2}$$

$$\begin{bmatrix} \ddot{\phi} \\ \ddot{\theta} \\ \ddot{\psi} \end{bmatrix} = \begin{bmatrix} (b_1 r + b_2 p)q + b_3(L_a + L_t) + b_4(N_a + N_t) \\ b_5 pr - b_6(p^2 - r^2) + b_7(M_a + M_t) \\ (b_8 p - b_2 r)q + b_4(L_a + L_t) + b_9(N_a + N_t) \end{bmatrix}, \tag{3}$$

where the inertial terms are defined as constants b_i:

$$\begin{bmatrix} b_1 \\ b_2 \\ b_3 \\ b_4 \\ b_8 \\ b_9 \end{bmatrix} = \frac{1}{I_x I_z - I_{xz}^2} \begin{bmatrix} (I_y - I_z)I_z - I_{xz}^2 \\ (I_x - I_y + I_z)I_{xz} \\ I_z \\ I_{xz} \\ (I_x - I_y)I_x + I_{xz}^2 \\ I_x \end{bmatrix}, \quad \begin{bmatrix} b_5 \\ b_6 \\ b_7 \end{bmatrix} = \frac{1}{I_y} \begin{bmatrix} (I_z - I_x) \\ I_{xz} \\ 1 \end{bmatrix},$$

for $\ddot{\phi}, \ddot{\theta}$ and $\ddot{\psi}$ as the angular accelerations of the biplane quadrotor, m as the mass of the biplane quadrotor, u, v and w as linear velocity components, p, q and r as angular velocity components, and F_{ax}, F_{ay} and F_{az} as aerodynamic forces acting on the biplane quadrotor, T as the thrust, L_t, M_t, and N_t as the roll, pitch, and yaw moments, and L_a, M_a, and N_a as the roll pitch and yaw moments due to the applied aerodynamics forces.

In the quadrotor mode, the rate of change in the linear and angular velocity is low; we consider these zero in the translation subsystem. Also, we consider that no aerodynamics forces are acting on the biplane quadrotor. We considered the effect of the swinging slung load as a disturbance estimated by the nonlinear disturbance observer.

By using Euler (ψ, θ, ϕ) configuration, and Newton's second law of motion on (2), rotational matrix is defined to determine the translation dynamics in the inertial frame given for quadrotor mode as

$$m \begin{bmatrix} \ddot{x} \\ \ddot{y} \\ \ddot{z} \end{bmatrix} = \begin{bmatrix} 0 \\ 0 \\ mg \end{bmatrix} + \begin{bmatrix} c\phi c\psi & s\phi s\theta c\psi - c\phi s\psi & c\phi s\theta c\psi + s\phi s\psi \\ c\theta s\psi & s\phi s\theta s\psi + c\phi c\psi & c\phi s\theta s\psi - s\phi c\psi \\ -s\theta & s\phi c\theta & c\phi c\theta \end{bmatrix} \begin{bmatrix} 0 \\ 0 \\ -T \end{bmatrix}. \tag{4}$$

Using (1), (3) and (4) biplane dynamics with slung load in quadrotor mode are

$$\ddot{x} = -U_x \frac{T}{m_a} + d_x \tag{5}$$

$$\ddot{y} = -U_y \frac{T}{m_a} + d_y \tag{6}$$

$$\ddot{z} = -c\phi c\theta \frac{T}{m_a} + \frac{gm}{m_a} + d_z \tag{7}$$

$$\ddot{\phi} = (b_1 r + b_2 p)q + b_3 L_t + b_4 N_t \tag{8}$$

$$\ddot{\theta} = b_5 pr - b_6(p^2 - r^2) + b_7 M_t \tag{9}$$

$$\ddot{\psi} = (b_8 p - b_2 r)q + b_4 L_t + b_9 N_t, \tag{10}$$

where $U_x = c\phi s\theta c\psi + s\phi s\psi$, $U_y = c\phi s\theta s\psi + s\phi c\psi, d_x = -\ddot{r}\left(\frac{m_l}{m_a}\right)$, $d_y = \ddot{s}\left(\frac{m_l}{m_a}\right)$ and $d_z = g\frac{m_l(\zeta/L)}{m_a} + \frac{m}{m_a}\left(\frac{\ddot{r}r + \dot{r}^2 + \ddot{s}s + \dot{s}^2}{\zeta} + \frac{(\dot{r}r + \dot{s}\dot{s})^2}{\zeta^3}\right), \ddot{s}$ and $\ddot{r}$ are the acceleration of the slung load about y and x axis respectively, $m + m_l = m_a$ is the combined mass of the biplane quadrotor and slung load, $\dot{s}, \dot{r}$ and $\dot{\zeta}$ are the slung load velocity components.

For observer design, we assume that the disturbance and derivative of disturbance are bounded and the rate of change of the disturbance is slow.

$$||\dot{d}_p(t)|| \leqslant D_p, \quad ||\dot{d}_o(t)|| \leqslant D_o \; t > 0.$$

A nonlinear disturbance observer [32] for the biplane quadrotor position is

$$\begin{aligned} \dot{n}_p &= -L_p n_p - L_p\left(L_p\dot{P} + G + \tfrac{1}{m_a}U_p\right), \\ \hat{d}_p &= n_p + L_p\dot{P}, \end{aligned} \tag{11}$$

where $U_p = R(O)E_3U_1, \hat{d}_p$ is the disturbance estimation, n_p is the observer state vector. $L_p > 0$ are the tunable gain matrices, $G = [0\ 0\ -g]^T, m_a$ is the mass of the biplane and slung load combined. Based on the desired trajectory given to mode selector, backstepping control strategy is applied for tracking.

3. Observer based Controller Design

Next, we design an observer-based controller for all modes of the quadrotor biplane, using the backstepping technique.

3.1. Quadrotor Mode

In the quadrotor mode, there are no aerodynamic forces acting on the vehicle. The augmented dynamics along with slug load given in (5)–(10), and written as

$$\begin{bmatrix} \dot{x}_1 \\ \dot{x}_2 \\ \dot{x}_3 \\ \dot{x}_4 \\ \dot{x}_5 \\ \dot{x}_6 \\ \dot{x}_7 \\ \dot{x}_8 \\ \dot{x}_9 \\ \dot{x}_{10} \\ \dot{x}_{11} \\ \dot{x}_{12} \end{bmatrix} = \begin{bmatrix} x_2 \\ (b_1x_6 + b_2x_2)x_4 + b_3L_t + b_4N_t + d_\phi \\ x_4 \\ b_5x_2x_6 - b_6(x_2^2 - x_6^2) + b_7M_t + d_\theta \\ x_6 \\ (b_8x_2 - b_2x_6)x_4 + b_4L_t + b_9N_t + d_\psi \\ x_8 \\ g\frac{m}{m_a} - \frac{T}{m_a}cx_1cx_3 + d_z \\ x_{10} \\ -\frac{T}{m_a}U_x + d_x \\ x_{12} \\ -\frac{T}{m_a}U_y + d_y \end{bmatrix}. \tag{12}$$

As shown in Fig. 2, three types of disturbances act on the biplane quadrotor, and are selected as per the mode. The slung load is only considered when biplane is in quadrotor mode. Wind gusts and partial rotor failures are applied on biplane in all three modes. Partial rotor failure is considered as a disturbance and calculated by the difference between reference propulsion system and nominal propulsion system of biplane quadrotor.

The dynamics of the roll subsystem are

$$\begin{aligned} \dot{x}_1 &= x_2 \\ \dot{x}_2 &= (b_1x_6 + b_2x_2)x_4 + b_3L_t + b_4N_t + d_\phi. \end{aligned} \tag{13}$$

As in (11), a nonlinear observer for the roll subsystem can be designed as

$$\begin{aligned} \dot{n}_\phi &= -L_\phi\left(n_\phi + L_\phi\dot{x}_1 + (b_1x_6 + b_2x_2)x_4 + b_3L_t + b_4N_t\right), \\ \hat{d}_\phi &= n_\phi + L_\phi x_2. \end{aligned} \tag{14}$$

Differentiating the estimated disturbance in roll subsystem, $\hat{d}_\phi$, we get

$$\begin{aligned} \dot{\hat{d}}_\phi &= \dot{n}_\phi + L_\phi\dot{x}_2 = -L_\phi n_\phi - L_\phi\left(L_\phi\dot{x}_1 + (b_1x_6 + b_2x_2)x_4 + b_3L_t + b_4N_t\right) \\ &\quad + L_\phi\left((b_1x_6 + b_2x_2)x_4 + b_3L_t + b_4N_t + d_\phi\right) \\ &= -L_\phi\left(n_\phi + L_\phi x_2\right) + L_\phi d_\phi = -L_\phi\hat{d}_\phi + L_\phi d_\phi = -L_\phi\tilde{d}_\phi, \end{aligned} \tag{15}$$

where $\tilde{d}_\phi = d_\phi - \hat{d}_\phi$ is the error, and $L_\phi > 0$ is a tuneable observer gain. For roll subsystem, error in roll angle is defined as $e_1 = x_1 - x_{1d}$ and for a positive definite function $V_1 = \frac{1}{2}e_1^2$, we get

$$\dot{V}_1 = e_1\dot{e}_1 = e_1(\dot{x}_1 - \dot{x}_{1d}) = e_1(x_2 - \dot{x}_{1d}),$$

with $k_1 > 0$. To satisfy this condition, a virtual control $x_{2d} = \dot{x}_{1d} - k_1e_1$ is designed such that $e_2 = x_2 - x_{2d} = x_2 - \dot{x}_{1d} + c_1e_1$, and so we get

$$\dot{V}_1 = e_1((e_2 + \dot{x}_{1d} - k_1e_1) - \dot{x}_{1d}) = e_1e_2 - k_1e_1^2. \tag{16}$$

The next step is to enhance the function V_1 with $e_2 = x_2 - x_{2d}$ and the error dynamics $\dot{e}_2 = \dot{x}_2 - \ddot{x}_{1d} + k_1\dot{e}_1$. Lyapunov positive definite function is given as

$$V_2 = V_1 + \frac{1}{2}e_2^2 + \frac{1}{2L_\phi}\tilde{d}_\phi^2.$$

By taking the first time derivative, and then using (15) and (16), we get

$$\begin{aligned} \dot{V}_2 &= e_1e_2 - k_1e_1^2 + e_2\left((b_1x_6 + b_2x_2)x_4 + b_3L_t + b_4N_t + d_\phi\right) \\ &\quad - \frac{1}{L_\phi}\dot{\hat{d}}_\phi\tilde{d}_\phi. \end{aligned} \tag{17}$$

Using (15) and (17), the control law is defined as

$$L_t = \frac{1}{b_3}\left(-e_1 - e_2k_2 + \ddot{x}_{2d} - k_1\dot{e}_1 - (b_1x_6 - b_2x_2)x_4 - b_4N_t - \hat{d}_\phi\right), \tag{18}$$

so that $\dot{V}_2 = -k_1e_1^2 - k_2e_2^2 - \tilde{d}_\phi^2 \leqslant 0,\ k_1, k_2 > 0$. Using the same calculation procedure, control laws for the pitch, yaw, altitude and position subsystem are

$$M_t = \frac{1}{b_7}\left(-e_3 - k_4e_4 + \ddot{x}_{3d} - \dot{e}_3k_3 - b_5x_2x_6 + b_6(x_2^2 - x_6^2) - \hat{d}_\theta\right), \tag{19}$$

$$N_t = \frac{1}{b_9}\left(-e_5 - k_6e_6 + \ddot{x}_{5d} - \dot{e}_5k_5 - (b_8x_2 - b_2x_6)x_4 - b_4L_t - \hat{d}_\psi\right), \tag{20}$$

$$T = \frac{m_a}{cx_1cx_3}\left(e_7 + k_8e_8 - \ddot{x}_{7d} + \dot{e}_7k_7 + g\frac{m}{m_a} - \hat{d}_z\right), \tag{21}$$

$$U_x = \frac{m_a}{T}\left(e_9 + k_{10}e_{10} - \ddot{x}_{9d} + \dot{e}_9k_9 - \hat{d}_x\right), \tag{22}$$

$$U_y = \frac{m_a}{T}\left(e_{11} + k_{12}e_{12} - \ddot{x}_{11d} + \dot{e}_{11}k_{11} - \hat{d}_y\right), \tag{23}$$

where $k_i > 0, i = 1, \ldots, 12$. Biplane quadrotor flies in the quadrotor mode while traveling to deliver a payload. After delivery, it is commanded to transition and switch from quadrotor to level flight mode to return in (i) lesser time and (ii) consuming lesser energy than the quadrotor. In addition, it can deliver more than one payload on a single flight.

3.2. Transition Mode

Transition maneuver allows the biplane quadrotor to switch a quadrotor mode to level flight mode. Initial command is to rotate about pitch axis at $\approx 90^\circ$. The primary stage of transition is governed by the quadrotor mode controller, and the last stage by the level flight controller. The dynamics in transition mode is same as the quadrotor mode but aerodynamics forces and moments are added.

The control laws include aerodynamics forces $[F_{ax}F_{ay}F_{az}]$ and moments $[L_aM_aN_a]$, and for $k_i > 0, i = 1, \ldots, 12$ are given as

$$\begin{aligned} L_t &= \tfrac{1}{b_3}\left(-e_1 - e_2k_2 + \ddot{x}_{2d} - k_1\dot{e}_1 - f_1 + b_3L_a - b_4(N_a + N_t) - \hat{d}_\phi\right), \\ M_t &= \tfrac{1}{b_7}\left(\ddot{x}_{3d} - e_3 - k_4e_4 - \dot{e}_3k_3 - b_5x_2x_6 + f_2 - \hat{d}_\theta\right) - M_a, \\ N_t &= \tfrac{1}{b_9}\left(-e_5 - k_6e_6 + \ddot{x}_{5d} - \dot{e}_5k_5 - f_3 - b_4(L_a + L_t) - b_9N_a - \hat{d}_\psi\right), \\ T &= \tfrac{m}{cx_1cx_3}\left(e_7 + k_8e_8 - \ddot{x}_{7d} + \dot{e}_7k_7 + g - \tfrac{F_{az}}{m} - \hat{d}_z\right), \\ U_x &= \tfrac{m}{T}\left(e_9 + k_{10}e_{10} - \ddot{x}_{9d} + \dot{e}_9k_9 - -\tfrac{F_{ax}}{m} - \hat{d}_x\right), \\ U_y &= \tfrac{m}{T}\left(e_{11} + k_{12}e_{12} - \ddot{x}_{11d} + \dot{e}_{11}k_{11} - \tfrac{F_{ay}}{m} - \hat{d}_y\right). \end{aligned}$$

3.3. Fixed wing Mode

Dynamics of the biplane quadrotor for the fixed wing mode is same as a fixed wing aircraft. Variables defined in dynamic equations of biplane quadrotor concern the quadrotor axis. It can be transformed from quadrotor axis to fixed-wing axis:

$$\begin{bmatrix} V_x \\ V_y \\ V_z \end{bmatrix}_W = \begin{bmatrix} -V_z \\ V_y \\ V_x \end{bmatrix}_Q = R_Q^W \begin{bmatrix} V_x \\ V_y \\ V_z \end{bmatrix}_Q, \; R_Q^W = \begin{bmatrix} 0 & 0 & -1 \\ 0 & 1 & 0 \\ 1 & 0 & 0 \end{bmatrix}.$$

Next, for $b_{w1} = I_{xz}(I_y + I_{xz})/B, b_{w2} = I_z^2/B, b_{w3} = I_{xz}(I_x + I_y)/B, b_{w4} = I_x I_y/B, b_{w5} = I_{xz}/B, b_{w6} = I_z/B, b_{w7} = 1/I_y, b_{w8} = I_x/I_y, b_{w9} = I_z/I_y, b_{w10} = I_{xz}/I_y, b_{w11} = I_x^2/B, b_{w12} = I_{xz}(I_y - I_{xz})/B, b_{w13} = I_x/B$ and $B = I_x I_z - I_{xz}^2$, the dynamics of the level flight mode are given by using above equation and [45] as

$$\dot{x} = c\theta c\psi u + (s\phi s\theta c\psi - c\phi s\psi)v + (c\phi s\theta c\psi + s\phi s\psi)w, \tag{24}$$

$$\dot{y} = c\theta s\psi u + (s\phi s\theta s\psi + c\phi c\psi)v + (c\phi s\theta s\psi - s\phi c\psi)w, \tag{25}$$

$$\dot{z} = -us\theta + vs\phi c\theta + wc\phi c\theta, \tag{26}$$

$$\dot{u} = \frac{F_{ax}}{m_a} - gs\theta + pv - qu + \frac{T}{m_a} + d_x, \tag{27}$$

$$\dot{v} = \frac{F_{ay}}{m} + gc\theta s\phi + pw - ru + d_y, \tag{28}$$

$$\dot{w} = \frac{F_{az}}{m} + gc\theta c\phi + rv - qw + d_z, \tag{29}$$

$$\dot{p} = -pq(b_{w3} + b_{w9}) - qr(b_{w11} - b_{w12}) - b_{w13}(L_a + L_t) + b_{w5}(N_a + N_t) + d_\phi, \tag{30}$$

$$\dot{q} = b_{w8}r^2 + b_{w9}p^2 + 2b_{w10}pr + b_{w7}(M_t + M_a) + d_\theta,$$

$$\dot{r} = pq(b_{w1} + b_{w2}) + qr(b_{w3} - b_{w4}) + b_{w5}(L_t + L_a) - b_{w6}(N_t + N_a) + d_\psi, \tag{31}$$

$$\dot{\phi} = p + qs\phi t\theta + rc\phi t\theta,$$

$$\dot{\theta} = qc\phi - rs\phi, \tag{32}$$

$$\dot{\psi} = q\frac{s\phi}{c\theta} + r\frac{c\phi}{c\theta}. \tag{33}$$

For the roll angle subsystem, the error between desired and actual roll angle is

$$e_\phi = \phi - \phi_d. \tag{34}$$

A positive definite function is defined as $V_{FM_\phi} = \frac{1}{2}e_\phi^2$ and taking time derivative of it and using (31), we get the desired roll angle rate

$$\dot{V}_{FM_\phi} = e_\phi\left(p + qs\phi t\theta + rc\phi t\theta - \dot{\phi}_d\right), \tag{35}$$

So control law can be defined for the desired roll angle rate p_d as

$$p_d = -k_\phi e_\phi - qs\phi t\theta - rc\phi t\theta + \dot{\phi}_d. \tag{36}$$

Error between roll angle rate is given by $e_p = p - p_d$ and positive definite function is defined as $V_{FM_p} = V_{FM_\phi} + \frac{1}{2}e_p^2 + \frac{1}{2L_\phi}\tilde{d}_\phi^2$. Taking time derivative, we get

$$\dot{V}_{FM_p} = e_p(-qr(b_{w11} - b_{w12}) - b_{w13}(L_a + L_t) + b_{w5}(N_a + N_t)) + e_p(-pq(b_{w3} + b_{w9}) + d_\phi - \dot{p}_d) - k_\phi e_\phi^2 + e_\phi e_p - \frac{1}{L_\phi}\tilde{d}_\phi\dot{\hat{d}}_\phi. \tag{37}$$

As explained in the quadrotor mode (15), (18), the roll angle rate control law is given as

$$L_t = \frac{1}{b_{w13}}\left(k_p e_p - pq(b_{w3} + b_{w9}) + qr(b_{w12} - b_{w11}) + b_{w5}(N_a + N_t) + \hat{d}_\phi + e_\phi - \dot{p}_d\right), \tag{38}$$

such that $\dot{V}_{FM_p} = -k_\phi^2 e_\phi^2 - k_p e_p^2 - \tilde{d}_\phi^2$ which guarantees asymptotic stable system for appropriately chosen $k_p > 0$.

The control laws for the pitch and yaw subsystem and the thrust are

$$M_t = \frac{-1}{b_{w7}}\left(k_q e_q + b_{w8}r^2 + b_{w9}p^2 + 2prb_{w10} + b_{w7}M_a - \dot{q}_d - e_\theta + \hat{d}_\theta\right), \tag{39}$$

$$N_t = \frac{1}{b_{w6}}(k_r e_r + pq(b_{w1} + b_{w2}) + qr(b_{w3} - b_{w4}) + b_{w5}(L_t + L_a) - b_{w6}N_a + e_\psi - \dot{r}_d + \hat{d}_\psi). \tag{40}$$

$$T = m_a\left(k_u e_u - \frac{F_{ax}}{m_a} + gs\theta - pv + qu - \hat{d}_z - e_u + \dot{u}_d\right), \tag{41}$$

By using (40), we rewrite (38) as

$$L_t = \frac{b_{w6}}{b_{w6}b_{w13} - b_{w5}^2}\left(-pq(b_{w3} + b_{w4}) - qr(b_{w11} - b_{w12}) + k_p e_p - \dot{p}_d + e_\phi\hat{d}_\phi\right) + \frac{b_{w5}}{b_{w6}b_{w13} - b_{w5}^2}\left(pq(b_{w1} + b_{w2}) + qr(b_{w3} + b_{w4}) + k_r e_r - \dot{r}_d + e_\psi\hat{d}_\psi\right) - L_a, \tag{42}$$

for tunable gains k_q, k_r and $k_u > 0$.

Desired pitch and yaw angle [45] are given as

$$\theta_d = \sin^{-1}\left(\frac{\dot{z}_d - k_z(z - z_d)}{\sqrt{a^2 + b^2}}\right) + \tan^{-1}\left(\frac{u}{vs\phi + wc\phi}\right), \; \psi_d = tan^{-1}\left(\frac{\dot{y}_d - k_y(y_d - y)}{\dot{x}_d + k_x(x_d - x)}\right) \tag{43}$$

where z_d is desired altitude, x_d and y_d are desired x and y positions, k_x, k_y, k_ϕ and k_z are tunable gains. We consider roll angle as a linear function of yaw angle, given as

$$\phi_d = k_\phi(\psi - \psi_d). \tag{44}$$

3.4. Control Allocation

First, we consider a fixed pitch propulsion system used in quadrotor biplane. The relation between the motor speed and the controller output is given as

$$\begin{bmatrix} T \\ L_t \\ M_t \\ N_t \end{bmatrix} = \underbrace{\begin{bmatrix} k & k & k & k \\ -kl & kl & kl & -kl \\ -kl & -kl & kl & -kl \\ -d & d & -d & d \end{bmatrix}}_{\delta} \begin{bmatrix} \Omega_1^2 \\ \Omega_2^2 \\ \Omega_3^2 \\ \Omega_4^2 \end{bmatrix}, \tag{45}$$

where k, d, and l are the lift and drag coefficients, and the arm length of the biplane quadrotor, respectively. We calculate the speed of the individual motors, by taking the inverse of the δ matrix, such as

$$\begin{bmatrix} \Omega_1^2 \\ \Omega_2^2 \\ \Omega_3^2 \\ \Omega_4^2 \end{bmatrix} = \begin{bmatrix} k & k & k & k \\ -kl & kl & kl & -kl \\ -kl & -kl & kl & -kl \\ -d & d & -d & d \end{bmatrix}^{-1} \begin{bmatrix} T \\ L_t \\ M_t \\ N_t \end{bmatrix}. \tag{46}$$

For a partial rotor failure, we consider a reference mode and nominal model for speed change using (46). By taking a difference with the reference system, we get the change in thrust and moments using (45). It is considered the disturbance and estimated by the design nonlinear observer and eliminated by the backstepping controller.

Table 1
Biplane quadrotor parameters.

Parameters	Value	Parameters	Value
g	9.8 ms^{-2}	Wing area (single)	0.754m^2
Mass (m)	12 kg	Aspect ratio	6.9
I_{xx}	1.86 $kg \cdot m^2$	Wing Span	2.29 m
I_{yy}	2.03 $kg \cdot m^2$	Gap-to-chord ratio	2.56
I_{zz}	3.617 $kg \cdot m^2$	slung load mass (m_l)	2 kg

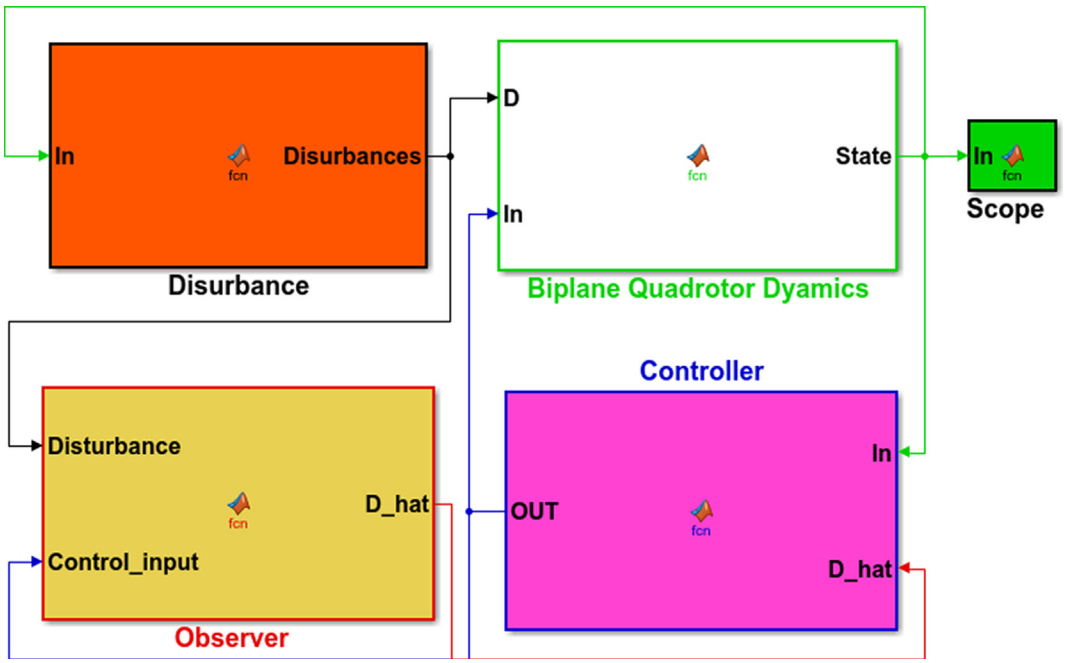

Fig. 4. MATLAB Simulink Model.

4. Results and discussion

Simulation is carried out by using the MATLAB Simulink. In simulation of the biplane quadrotor with slung load, wing gust and partial rotor failure. Biplane parameters with slung load is given in Table 1.

Initially the biplane quadrotor position [xyz] is [0.550.1] and attitude [$\phi\theta\psi$] is [000]. Biplane is take off during t = 0 – 20 sec and then fly with 4 m/s speed up to t = 294 s and then it commanded to land in between t = 294 – 314 sec.

Fig. 4 Shows the Simulink model of the proposed control architecture.

Fig. 5 show the $x-y$ position and altitude of the quadrotor biplane with slung load during the whole flight envelop. There is a very small fluctuation in y and z axis due to the swinging of the slung load. It shows the effectiveness of the designed observer and controller.

Fig. 6 shows attitude tracking during the whole flight envelope. It can be observed that there is a small oscillation in the roll and pitch angle because of the fluctuation in the $x-y$ position of the biplane quadrotor due to the slung load and yaw angle is independently controlled by the control law.

Disturbance observer performance is shown in Fig. 7. The observer effectively tracks the disturbance generated in the position subsystem due to the slung load swinging.

Fig. 8 show the $x-y$ position and altitude tracking of the biplane quadrotor with slung load in the presence of the wing gust. Slung load swing more due to the wind gust so there is a small steady state error in the y axis. there is a no significant error in altitude and x position these shows that designed controller is capable to handle the disturbance and track the desired trajectory.

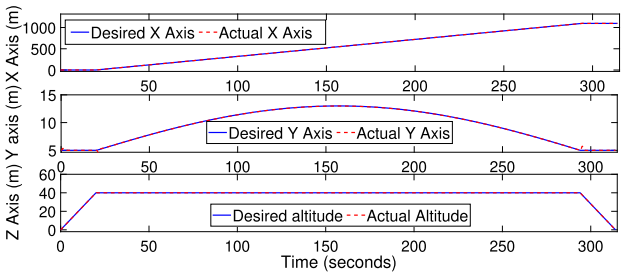

Fig. 5. Altitude and Position tracking with slung load.

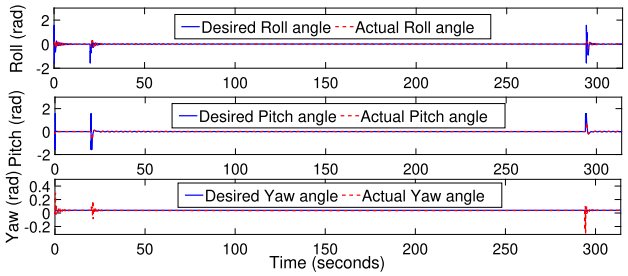

Fig. 6. Attitude Tracking with Slung Load.

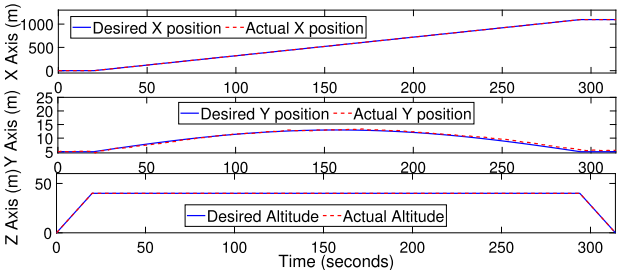

Fig. 8. Position and altitude tracking of Biplane quadrotor with slung load in the presence of wind gust.

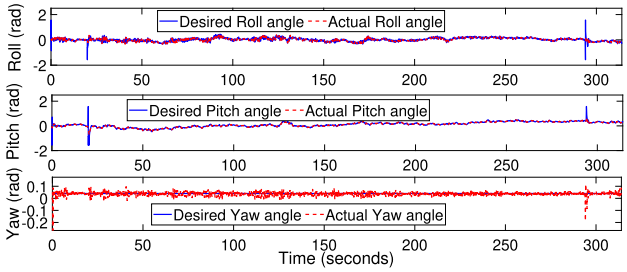

Fig. 9. Attitude tracking of Biplane quadrotor with slung load in the presence of wing gust.

Attitude tracking of the biplane quadrotor with slung load despite wind gusts is shown in Fig. 9. There are small fluctuations in the all three angles due to the wind gust and slung load swinging. The proposed observer based controller handles the disturbances. Disturbance observer performance with wind gust applied on biplane quadrotor and the slung load, is shown in Figs. 10 and 11.

Position and attitude tracking of the biplane quadrotor with the slung load and partial rotor failure is shown Figs. 12 and 13.

There is a small error in y and z axis, and a more significant error while landing due to the partial rotor failure, but the controller ensures safe landing. There are small fluctuations in roll and yaw angles. Disturbance observer performance for position and attitude subsystems are shown in Fig. 14 and 15.

Next, simulation is carried out for the quadrotor mode and the transition mode. When the biplane drops the payload, it is commanded to perform the transition mode to switch the quadrotor mode to level flight mode.

4.1. Quadrotor Mode and Transition Mode

We consider that in $t = 0 - 30$ sec, the biplane takes off, during $t = 30 - 50$ sec it is in hovering state and at $t = 50 - 53$ sec, transition mode is initiated. Wind gust is applied from the beginning of

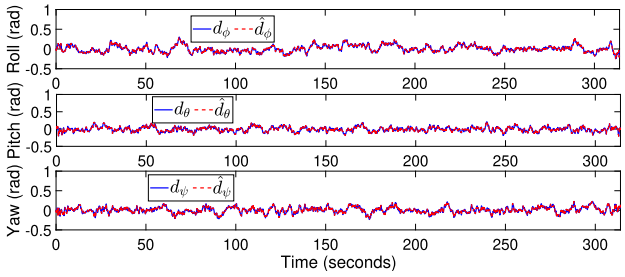

Fig. 10. Disturbance due to the slung load in the presence of wing gust in attitude subsystem.

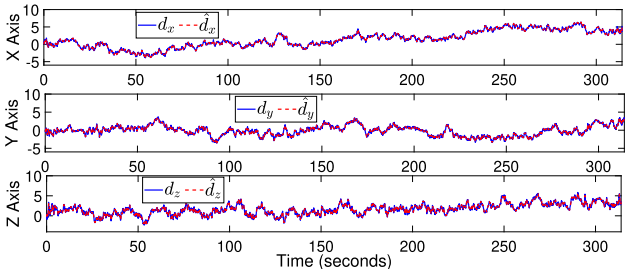

Fig. 11. Disturbance due to the slung load in the presence of wing gust in position subsystem.

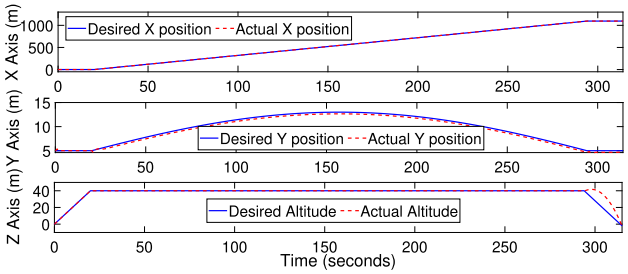

Fig. 12. Position and altitude tracking of biplane with slung load and partial rotor failure.

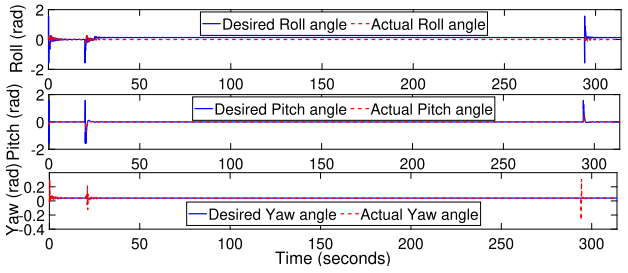

Fig. 13. Attitude tracking of biplane with slung load in the presence of partial rotor failure.

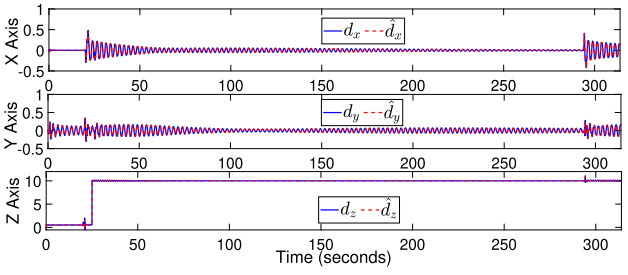

Fig. 14. Disturbance in position subsystem with slung load by a partial rotor failure.

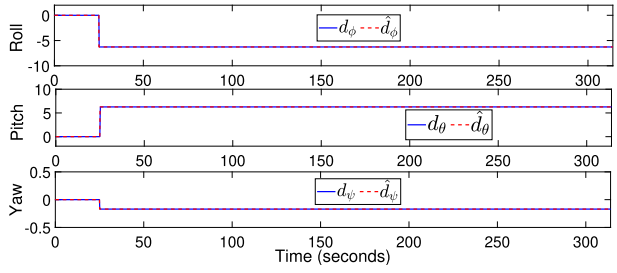

Fig. 15. Disturbance generated in attitude with slung load by a partial rotor failure.

simulation and rotor partial failure is applied during transition. Altitude and position tracking during the quadrotor and transition mode under these conditions are shown in Fig. 16.

There is a small oscillation in the $x-y$ position and negligible error generated in the altitude. At $t = 50$ sec, transition maneuver is initiated and at the same time partial rotor failure is introduced. Because of the partial rotor, there is a small error generated in the altitude subsystem. During transition, we cannot control the $x-y$ position that is why there is a error generated. So we can say that, designed observer based controller is effectively tackle the disturbance and partial rotor failure and able to tracked the desired trajectory.

Fig. 17 shows the attitude tracking during quadrotor and transition mode with wind gust and partial rotor failure. There is a small fluctuation during the quadrotor mode due to wind gust, and the transition mode with partial rotor failure at $t = 50$ sec, effectively reduces pitch angle while maintaining the roll and yaw angle around zero. It shows effectiveness of the controller and observer.

Observer performance during the quadrotor and transition mode with wind gust and partial rotor failure in position and attitude subsystems are shown in Fig. 18 and Fig. 19. Designed observer effectively tracks the disturbance.

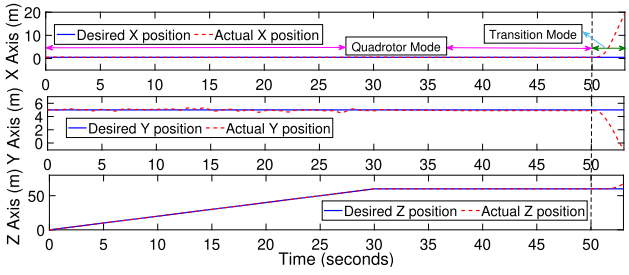

Fig. 16. Altitude and position tracking during quadrotor and transition mode.

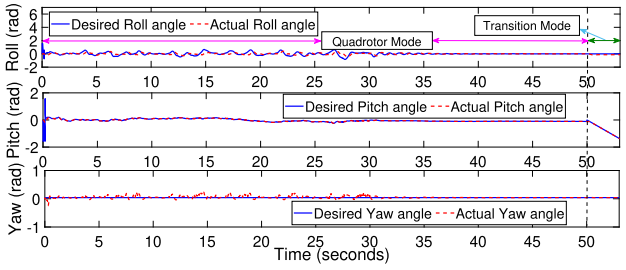

Fig. 17. Attitude tracking during quadrotor and transition mode.

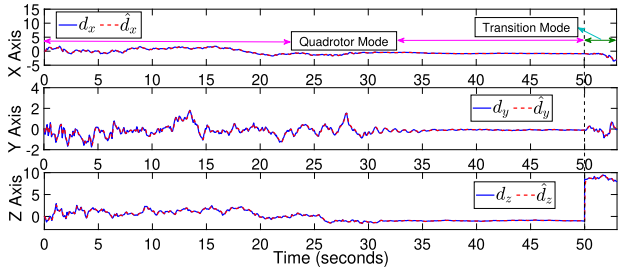

Fig. 18. Disturbance by the wind gust and partial rotor failure in position subsystem.

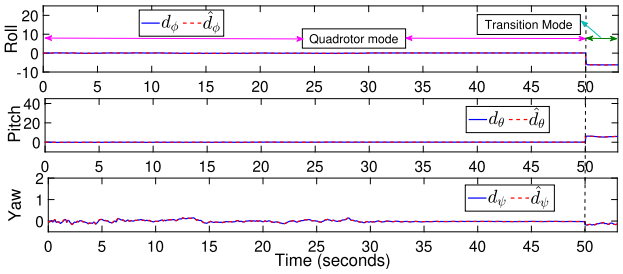

Fig. 19. Disturbance by the wind gust and partial rotor failure in attitude subsystem.

4.2. Fixed wing mode with disturbance and partial rotor failure

In this section, simulation is carried out for the fixed wing mode of the quadrotor biplane with the wind gust and partial rotor failure to check the efficiency of the design observer based backstepping controller. First simulation is carried out for the partial rotor failure and the combine with the wind gust. So for the partial rotor failure, simulation is carried out for the 100 s in which after $t = 50$sec, partial rotor failure is introduced and biplane commanded to fly with 15 m/s sec velocity while maintain y axis and altitude at 30 m height. Figs. 20 and 21 show the position, altitude and attitude tracking of the biplane in fixed wing mode in the presence of the rotor failure.

We observe small fluctuations in the y axis but negligible changes in the $x-z$ axis due to the rotor failure. There is a small change also in the yaw and roll angle because of it but overall biplane is able to track the desired trajectory with small deflection in the y axis and small disturbance in roll and yaw angle. Nonlinear disturbance observer performance is shown in Fig. 22 and Fig. 23 for the position, altitude and attitude subsystem. It can be seen that agility and effectiveness of the observer is good.

Wind gust is applied with partial rotor failure while biplane is in fixed wing mode. Figs. 24 and 25 shows the attitude and position tracking in the presence of wind gust and at $t = 50$ sec, rotor failure is applied.

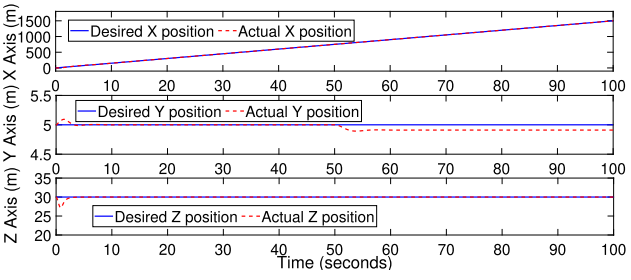

Fig. 20. Position and altitude tracking in fixed wing mode with partial rotor failure.

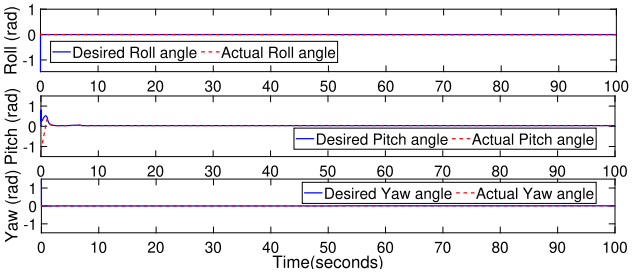

Fig. 21. Attitude tracking in the fixed wing mode with partial rotor failure.

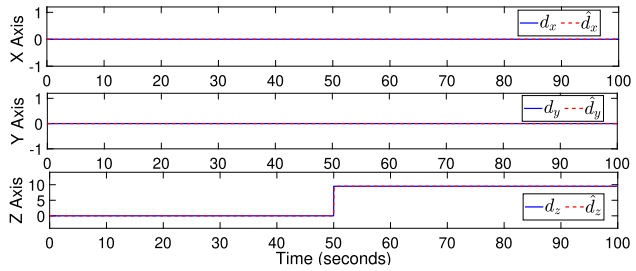

Fig. 22. Observer Performance about position, altitude in fixed wing mode while rotor fails.

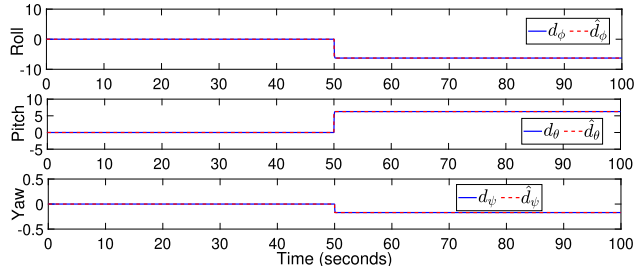

Fig. 23. Observer Performance about attitude in the fixed wing mode while rotor failure.

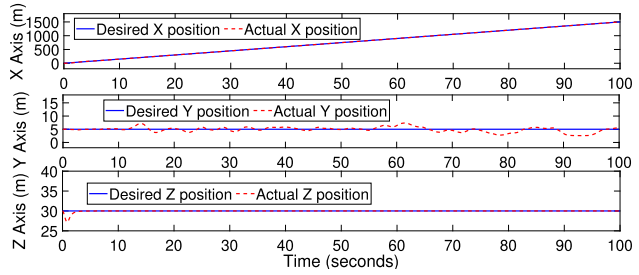

Fig. 24. Position and Altitude tracking in the presence of wind gust and rotor failure.

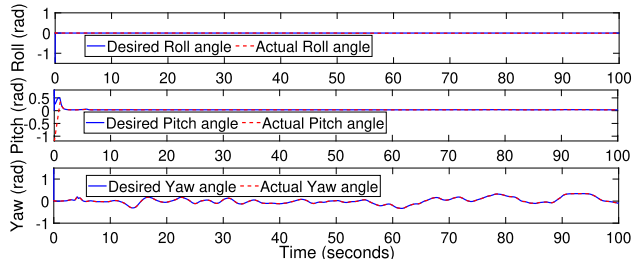

Fig. 25. Attitude tracking in the presence of wind gust and rotor failure.

Wind gusts result in small fluctuations in the *y* axis and yaw angle. Biplane tracks the altitude and *x* axis position amidst external disturbance, showing the effectiveness of the observer based backstepping controller.

Observer performance in disturbance tracking is shown in Figs. 26 and 27. The designed observer effectively tracks the disturbance. When partial rotor failure is introduced, there is a spike in the altitude and altitude of the biplane at t = 50 s, but tracking is achieved with small delay.

In this simulation study, we design an observer-based backstepping controller for the biplane quadrotor with slung load, and it is also capable of handling partial rotor failure. This algorithm can be implemented on the actual hardware using MATLAB Simulink and PX4 flight controller. Possible challenges are:

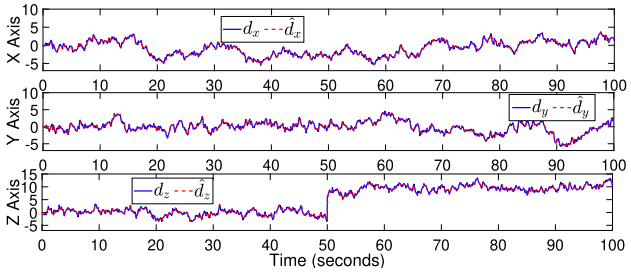

Fig. 26. Disturbance performance for the position subsystem in fixed-wing mode.

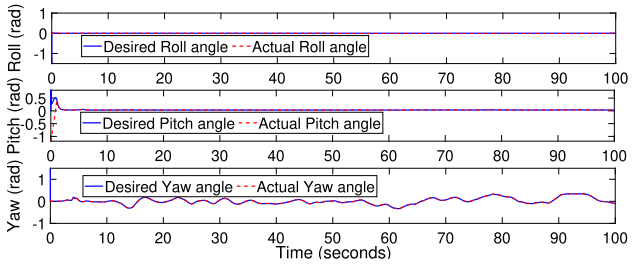

Fig. 27. Disturbance performance for the attitude subsystem in fixed-wing mode.

- Sampling time: In this simulation study, we set sampling time as 0.01 sec, but that may change according to the hardware.
- Availability of onboard sensors.
- It is hard to implement partial rotor failure to test these algorithms in the actual hardware.
- It is challenging to predict the behavior of the slung load in the presence of wind gusts in the real world.

5. Conclusions

This simulation study is divided into three parts: (i) Quadrotor biplane (only quadrotor mode) with slung load, wind gust, and partial rotor failure (ii) Quadrotor biplane (quadrotor and transition mode) without slung load but still wind gust, and partial rotor failure are there and (iii) fixed-wing mode with partial rotor failure and wind gust. Simulation is carried out for all these parts. The outcomes of this study are.

- Mathematical model of the biplane quadrotor with slung load is proposed.
- Design Nonlinear Observer based backstepping controller for the different disturbance combinations.
- This control architecture can handle any disturbance applied on the biplane quadrotor with a slung load.
- The proposed control scheme is also effective while biplane quadrotor performs transition maneuver during partial rotor failure.
- There is a minimal error generated in the trajectory tracking while fixed-wing mode of biplane quadrotor and in the presence of the wind gust and partial rotor failure.
- Nonlinear Observer based backstepping controller tracks the desired trajectory in the presence of the disturbances for all three modes.

Declaration of Competing Interest

The authors declare that they have no known competing financial interests or personal relationships that could have appeared to influence the work reported in this paper.

Acknowledgements

The publication of this article was funded by Qatar National Library.

References

[1] Hrishikeshavan V, Bogdanowicz C, Chopra I. Design, performance and testing of a quad rotor biplane micro air vehicle for multi role missions 2014;6 (3):sss 155–173. doi:10.1260/1756-8293.6.3.155.
[2] Swarnkar S, Parwana H, Kothari M, Abhishek A. Biplane-quadrotor tail-sitter UAV: Flight dynamics and control 2018;41(5):1049–67. doi: https://doi.org/10.2514/1.g003201.
[3] Chipade VS, Abhishek M, Kothari RR. Chaudhari. Systematic design methodology for development and flight testing of a variable pitch quadrotor biplane VTOL UAV for payload delivery 2018;55:94–114. doi: https://doi.org/10.1016/j.mechatronics.2018.08.008.
[4] Reddinger JP, McIntosh K, Zhao D, Mishra S. Modeling and trajectory control of a transitioning quadrotor biplane tailsitter. In: Vertical Flight Society 75th Annual Forum, Vol. 93; 2019.
[5] Ryseck P, Yeo D, Hrishikeshavan V, Chopra I. Aerodynamic and mechanical design of a morphing winglet for a quadrotor biplane tail-sitter; 2019.
[6] Ryseck P, Yeo DW, Hrishikeshavan V, Chopra I. Expanding the mission capabilities of a quadrotor biplane tail-sitter with morphing winglets. American Institute of Aeronautics and Astronautics 2020. doi: https://doi.org/10.2514/6.2020-1506.
[7] McIntosh K, Mishra S, Zhao D, Reddinger JPF. Optimal trajectory generation for a quadrotor biplane tailsitter; 2020.
[8] Bisgaard M, Bendtsen JD, la Cour-Harbo A. Modeling of generic slung load system. Journal of guidance, control, and dynamics 2009;32(2):573–85.
[9] Guerrero M, Mercado D, Lozano R, García C. Ida-pbc methodology for a quadrotor uav transporting a cable-suspended payload. In: 2015 International Conference on Unmanned Aircraft Systems (ICUAS). IEEE; 2015. p. 470–6.
[10] Bisgaard M, Bendtsen JD, la Cour-Harbo A. Modeling of generic slung load system 2009;32(2):573–85. doi: https://doi.org/10.2514/1.36539.
[11] Notter S, Heckmann A, Mcfadyen A, Gonzalez F. Modelling, simulation and flight test of a model predictive controlled multirotor with heavy slung load 2016;49 (17): 182–7. doi:10.1016/j.ifacol.2016.09.032.
[12] El-Ferik S, Syed AH, Omar HM, Deriche MA. Nonlinear forward path tracking controller for helicopter with slung load 2017;69:602–8. doi: https://doi.org/10.1016/j.ast.2017.07.028.
[13] Shirani B, Najafi M, Izadi I. Cooperative load transportation using multiple UAVs 2019;84:158–69. doi: https://doi.org/10.1016/j.ast.2018.10.027.
[14] Yu G, Cabecinhas D, Cunha R, Silvestre C. Nonlinear backstepping control of a quadrotor-slung load system. IEEE/ASME Trans. Mechatron. 2019;24 (5):2304–15. doi: https://doi.org/10.1109/TMECH.2019.2930211.
[15] de Angelis EL. Swing angle estimation for multicopter slung load applications 2019;89:264–74. doi: https://doi.org/10.1016/j.ast.2019.04.014.
[16] Cao Y, Nie W, Wang Z, Wan S. Dynamic modeling of helicopter-slung load system under the flexible sling hypothesis 2020;99:105770. doi: https://doi.org/10.1016/j.ast.2020.105770.
[17] Gao Z. On the centrality of disturbance rejection in automatic control. ISA Trans 53. doi:10.1016/j.isatra.2013.09.012.
[18] Besnard L, Shtessel YB, Landrum B. Quadrotor vehicle control via sliding mode controller driven by sliding mode disturbance observer 2012;349(2):658–84. doi: https://doi.org/10.1016/j.jfranklin.2011.06.031.
[19] Chen F, Lei W, Zhang K, Tao G, Jiang B. A novel nonlinear resilient control for a quadrotor UAV via backstepping control and nonlinear disturbance observer 2016;85(2):1281–95. doi: https://doi.org/10.1007/s11071-016-2760-y.
[20] Chovancová A, Fico T, Hubinský P, Duchoň F. Comparison of various quaternion-based control methods applied to quadrotor with disturbance observer and position estimator 2016;79:87–98. doi: https://doi.org/10.1016/j.robot.2016.01.011.
[21] Zhang Y, Liu J, He W. Disturbance observer design and vibration control for a flexible aircraft wing 2017;40(13):3760–73. doi: https://doi.org/10.1177/0142331217730887.
[22] Chen M, Xiong S, Wu Q. Tracking flight control of quadrotor based on disturbance observer. IEEE Transactions on Systems, Man, and Cybernetics: Systems 2021;51(3):1414–23. doi: https://doi.org/10.1109/TSMC.2019.2896891.
[23] Rodríguez-Mata AE, González-Hernández I, Rangel-Peraza JG, Salazar S, Leal RL. Wind-gust compensation algorithm based on high-gain residual observer to control a quadrotor aircraft: Real-time verification task at fixed point 2018;16(2):856–66. doi: https://doi.org/10.1007/s12555-016-0771-6.
[24] Madani T, Benallegue A. Sliding mode observer and backstepping control for a quadrotor unmanned aerial vehicles. In: American Control Conference, 2007. p. 5887–92. doi: https://doi.org/10.1109/ACC.2007.4282548.
[25] Zheng M, Lyu X, Liang X, Zhang F. A generalized design method for learning-based disturbance observer. IEEE/ASME Trans. Mechatron. 2021;26(1):45–54. doi: https://doi.org/10.1109/TMECH.2020.2999340.
[26] Lyu X, Zhou J, Gu H, Li Z, Shen S, Zhang F. Disturbance observer based hovering control of quadrotor tail-sitter vtol uavs using h_∞ synthesis. IEEE Robotics and Automation Letters 2018;3(4):2910–7. doi: https://doi.org/10.1109/LRA.2018.2847405.
[27] Li Z, Zhang L, Liu H, Zuo Z, Liu C. Nonlinear robust control of tail-sitter aircrafts in flight mode transitions 2018;81:348–61. doi: https://doi.org/10.1016/j.ast.2018.08.021.
[28] Smith J, Su J, Liu C, Chen W-H. Disturbance observer based control with anti-windup applied to a small fixed wing UAV for disturbance rejection 2017;88 (2–4):329–46. doi: https://doi.org/10.1007/s10846-017-0534-5.
[29] Castañeda H, Salas-Peña OS, de León-Morales J. Extended observer based on adaptive second order sliding mode control for a fixed wing UAV 2017;66:226–32. doi: https://doi.org/10.1016/j.isatra.2016.09.013.
[30] Shi D, Wu Z, Chou W. Harmonic extended state observer based anti-swing attitude control for quadrotor with slung load 2018;7(6):83. doi: https://doi.org/10.3390/electronics7060083.
[31] Zhang Z, Wang F, Guo Y, Hua C. Multivariable sliding mode backstepping controller design for quadrotor UAV based on disturbance observer 61 (11). doi:10.1007/s11432-017-9434-7.
[32] Dalwadi N, Deb D, Kothari M, Ozana S. Disturbance observer-based backstepping control of tail-sitter UAVs 2021;10(6):119. doi: https://doi.org/10.3390/act10060119.
[33] Hou Z, Lu P, Tu Z. Nonsingular terminal sliding mode control for a quadrotor UAV with a total rotor failure 2020;98:105716. doi: https://doi.org/10.1016/j.ast.2020.105716.
[34] Li B, Hu Q, Yang Y, Postolache OA. Finite-time disturbance observer based integral sliding mode control for attitude stabilisation under actuator failure 2019;13(1):50–8. doi: https://doi.org/10.1049/iet-cta.2018.5477.
[35] De Crousaz C, Farshidian F, Neunert M, Buchli J. Unified motion control for dynamic quadrotor maneuvers demonstrated on slung load and rotor failure tasks. In: 2015 IEEE International Conference on Robotics and Automation (ICRA). IEEE; 2015. p. 2223–9.
[36] Freddi A, Lanzon A, Longhi S. A feedback linearization approach to fault tolerance in quadrotor vehicles 2011;44(1):5413–8. doi: https://doi.org/10.3182/20110828-6-it-1002.02016.
[37] Lien Y-H, Peng C-C, Chen Y-H. Adaptive observer-based fault detection and fault-tolerant control of quadrotors under rotor failure conditions 2020;10 (10):3503. doi: https://doi.org/10.3390/app10103503.
[38] Merheb A-R, Noura H, Bateman F. Emergency control of ar drone quadrotor uav suffering a total loss of one rotor. IEEE/ASME Trans Mechatron 2017;22 (2):961–71. doi: https://doi.org/10.1109/TMECH.2017.2652399.
[39] Guzmán-Rabasa JA, López-Estrada FR, González-Contreras BM, Valencia-Palomo G, Chadli M, Pérez-Patricio M. Actuator fault detection and isolation on a quadrotor unmanned aerial vehicle modeled as a linear parameter-varying system 2019;52(9–10):1228–39. doi: https://doi.org/10.1177/0020294018824764.
[40] Sadeghzadeh I, Mehta A, Zhang Y. Fault/damage tolerant control of a quadrotor helicopter UAV using model reference adaptive control and gain-scheduled PID. Am Inst Aeronaut Astronaut 2011. doi: https://doi.org/10.2514/6.2011-6716.
[41] Chamseddine A, Zhang Y, Rabbath C-A, Apkarian J, Fulford C. Model reference adaptive fault tolerant control of a quadrotor UAV. Am Inst Aeronaut Astronaut 2011. doi: https://doi.org/10.2514/6.2011-1606.
[42] Lippiello V, Ruggiero F, Serra D. Emergency landing for a quadrotor in case of a propeller failure: A backstepping approach. In: IEEE/RSJ International Conference on Intelligent Robots and Systems, 2014. p. 4782–8. doi: https://doi.org/10.1109/IROS.2014.6943242.
[43] Lippiello V, Ruggiero F, Serra D. Emergency landing for a quadrotor in case of a propeller failure: A pid based approach. In: 2014 IEEE International Symposium on Safety, Security, and Rescue Robotics (2014). p. 1–7. doi: https://doi.org/10.1109/SSRR.2014.7017647.
[44] Zhou X, Liu R, Zhang J, Zhang X. Stabilization of a quadrotor with uncertain suspended load using sliding mode control. Am Soc Mech Eng 2016. doi: https://doi.org/10.1115/detc2016-60060.
[45] Ambati PR, Padhi R. A neuro-adaptive augmented dynamic inversion design for robust auto-landing. IFAC Proc Vol 2014;47(3):12202–7.
[46] Dalwadi Nihal, Deb Dipankar, Muyeen SM. Adaptive backstepping controller design of quadrotor biplane for payload delivery. IET Intelligent Transport Systems 2022:. In press10.1049/itr2.12171.

Nihal Dalwadi received his B.Tech in Instrumentation and control engineering from Sardar Vallabhbhai Patel Institute of Technology (SVIT), Vasad in 2013 and M. Tech degree in Control and Automation from Nirma University, Ahmedabad, India in 2016. He is PhD scholar in Institute of Infrastructure, Technology, Research And Management (IITRAM) and His research interests include control theory, adaptive control and nonlinear controller design for under-actuated systems.

Dipankar Deb is a Senior Member of IEEE and has served a couple of years at IIT Guwahati as an Assistant Professor (AGP 8000) during 2010–2012. He has over 6 years of Industrial experience both in New York (USA) and GE Global Research (Bengaluru) India. He received his Ph.D. from the University of Virginia, Charlottesville, USA (2007), and Masters from the University of Florida (2004). From July 2015 to Jan 2019, he has served as an Associate professor, and from Jan 24, 2019, onward he is a Professor in Electrical Engineering at the Institute of Infrastructure Technology Research and Management (IITRAM) Ahmedabad. He holds 6 US patents, 1 Indian Patent, and has published 40 Science Citation Indexed (SCI) Journal articles and 40 + International conference papers. He has also authored 11 books with reputed publishers like Springer and Elsevier. He is a Book Series Editor with Springer for a Book Series titled, ''Studies in Infrastructure and Control", and an Associate Editor for IEEE Access. He has worked extensively in areas such as Adaptive Control, Active flow control, Renewable Energy, Cognitive Robotics, and Machine Learning. He is recently listed in the top 2% of Researchers worldwide for 2020–21 as published by Stanford University.

Dr. S. M. Muyeen, a senior member of IEEE, received his B.Sc. Eng. Degree from Rajshahi University of Engineering and Technology (RUET), Bangladesh formerly known as Rajshahi Institute of Technology, in 2000 and M. Eng. and Ph.D. Degrees from Kitami Institute of Technology, Japan, in 2005 and 2008, respectively, all in Electrical and Electronic Engineering. At the present, he is working as an Associate Professor in the School of Electrical Engineering Computing and Mathematical Sciences, Curtin University, Australia. His research interests are power system stability and control, electrical machine, FACTS, energy storage system (ESS), Renewable Energy, and HVDC system. He has been a Keynote Speaker and an Invited Speaker at many international conferences, workshops, and universities. He has published more than 225 articles in different journals and international conferences. He has published seven books as an author or editor. He is serving as Editor/Associate Editor for many prestigious Journals from IEEE, IET, and other publishers including IEEE Transactions on Sustainable Energy, IEEE Transactions on Energy Conversion, IEEE Power Engineering Letters, IET Renewable Power Generation and IET Generation, Transmission & Distribution, etc. Dr. Muyeen is the senior member of IEEE and Fellow of Engineers Australia.